EPJ Web of Conferences **278**, 01002 (2023)
ISRD 17
https://doi.org/10.1051/epjconf/202327801002

Design Considerations for Boron-Diffused and Implanted 4H-SiC Epitaxial Neutron Detectors for Dosimetry and Monitoring Applications

Frank H. Ruddy[1,*], *Joshua W.* Kleppinger[2], and *Krishna C.* Mandal[2]

[1]Ruddy Consulting, 2162 Country Manor Dr., Mount Pleasant, South Carolina, USA
[2]Department of Electrical Engineering, University of South Carolina, Columbia, South Carolina, USA

Abstract. Thermal-neutron detectors based on 4H-SiC semiconductor and ^{10}B converter reactions have many advantages for neutron dosimetry and monitoring applications. These radiation-resistant detectors are capable of stable operation in elevated-temperature environments up to 700 °C for extended periods. The recent development of SiC detectors where the ^{10}B is incorporated into the detector by ion implantation or diffusion leads to interesting application-specific design possibilities. The design of boron-diffused detectors is discussed as well as ways to optimize their design.

1 Introduction

Neutron detectors based on Silicon Carbide (SiC) have many advantages for neutron dosimetry and monitoring applications [1]. Following the first demonstration of radiation detectors based on 4H-SiC epitaxial layers [2], rapid progress and refinement of SiC detectors have been achieved [3-7]. SiC neutron detectors are particularly useful for measurements in the high-temperature, high-radiation environments typically encountered in nuclear power applications [8]. The wide bandgap (3.27 eV at 300K) results in far fewer thermally generated charge carriers compared to conventional lower bandgap semiconductors such as silicon or germanium and allows operation in elevated-temperature environments up to 700 °C without the need for cooling. Furthermore, SiC radiation detectors are extremely radiation tolerant, and have been shown to be operational after gamma-ray doses up to 22.7 MGy (^{137}Cs) [9] and fast-neutron (E >1MeV) fluences up to 1.7 x 10^{17} cm^{-2}[10]. SiC detectors are particularly well suited to spent fuel monitoring applications as reported at previous symposia in this series [11-13].

2 Background

Like all neutron detectors, SiC detectors rely on detection of neutron-induced reaction products in the form of energetic ions, which can produce detectable ionization when they interact with the detector. SiC detectors based on boron neutron-convertor layers that have been implanted into the detector [14] or diffused into the detector [11] have been reported

[*] Corresponding author: FrankHRuddy@gmail.com

© The Authors, published by EDP Sciences. This is an open access article distributed under the terms of the Creative Commons Attribution License 4.0 (http://creativecommons.org/licenses/by/4.0/).

previously in this symposium series. In both cases, neutron-induced $^{10}B(n,\alpha)^{7}Li$ reaction products enter the active volume of the detector and produce ionization and detectable charge pulses.

The calculated [15] ranges in SiC for the ions produced in thermal neutron-induced ^{10}B reactions are summarized in Table 1. Thermal neutron reactions with ^{10}B atoms located

Table 1 Calculated Ranges in Silicon Carbide for ^{10}B Neutron-Induced Reaction Products

Particle	Energy (keV)	Range in SiC*
$^{10}B(n,\alpha)^{7}Li$ (480-keV excited state – 94%)		
α	1470	3.4 μm
^{7}Li	840	1.6 μm
$^{10}B(n,\alpha)^{7}Li$ (ground state – 6%)		
α	1777	4.14 μm
^{7}Li	1015	1.81 μm

more than 4.14 μm from the active volume of the detector are not detectable. The thermal-neutron induced reaction products from ^{10}B atoms located closer than 1.6 μm to the active volume are capable of reaching the active volume. If a sufficient amount of ionization is produced within the active volume, a signal corresponding to the neutron-induced reaction will be detected.

In the case of boron-implanted neutron detectors, a narrow layer of boron atoms will be produced at a depth corresponding to the range of the implanted boron atoms in the detector. Issa, *et al.* [14,16-18] have reported results for neutron detectors where 180-keV and 2-MeV boron ions were implanted in 2-μm and 4-μm aluminum contact layers, respectively, of SiC p-n diodes. The calculated projected ranges of the 180-keV and 2-MeV boron ions are 0.45 μm and 2.5 μm, respectively. Because the location of the boron atoms can be precisely controlled relative to the location of the detector active volume, it is possible to optimize the corresponding detector response. Detailed discussions of the detector-design issues and neutron-response results can be found in references [14] and [16-18].

In the case of boron-diffused detectors [11], boron (a p-type dopant) is diffused into n-type 4H-SiC to produce a p-n junction as depicted in Fig. 1. Under the influence of a reverse bias, the n-region is depleted of charge carriers and becomes the active volume of the detector as shown in Fig. 2. For the detector tested in reference [11], the thickness of the initial n-layer was 50 μm. Therefore, the thickness of the active volume of the fully depleted detector is 50 μm minus the distance of the p-n interface from the surface of the detector. Thermal-neutron interactions with ^{10}B atoms in the detector can produce energetic ^{4}He and ^{7}Li ions which produce ionization in the detector active volume as shown in Fig. 3. In the case shown in Fig.3, the location of the neutron reaction results in all of the energy of the ^{4}He and ^{7}Li being deposited within the active volume of the detector. Less energy may be deposited if the reaction occurs within the active volume but less than the range of either the ^{4}He or ^{7}Li ion from a boundary of the active volume or if the reaction occurs outside of the active volume. No ionization is expected to be produced in the detector active volume by $^{10}B(n,\alpha)^{7}Li$ reactions that originate from more than about 4.14 μm outside of the active volume. Therefore, if the peak boron concentration shown schematically in Fig. 3 is more than 4 μm from the p-n interface, the maximum ^{10}B concentration will not contribute to the detector response signal. Ideally, the peak boron concentration should be as close as possible to the p-n interface and not have a concentration that greatly exceeds the n-dopant (nitrogen)

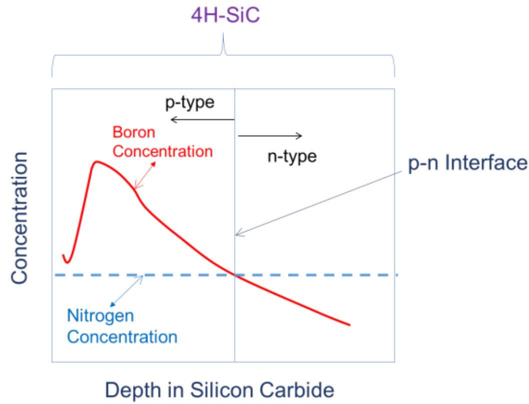

Fig. 1. Schematic representation of the regions of a p-n diode formed by diffusing boron into n-type SiC.

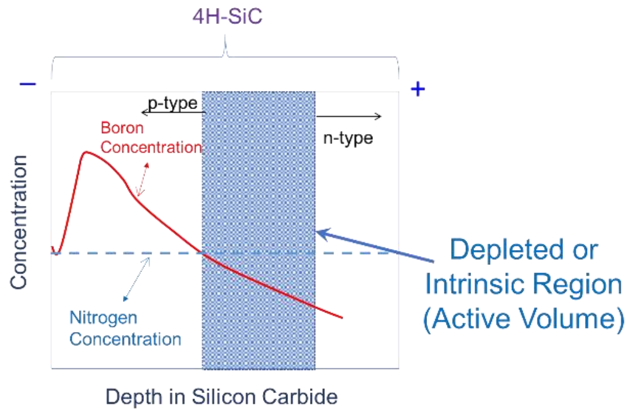

Fig. 2. Application of a reverse bias produces a depletion region, which acts as the active volume for the detector. A partially depleted detector is shown. The maximum depletion depth corresponds to the full thickness of the initial n^- region (distance from the p-n interface to the remainder of the epitaxial layer).

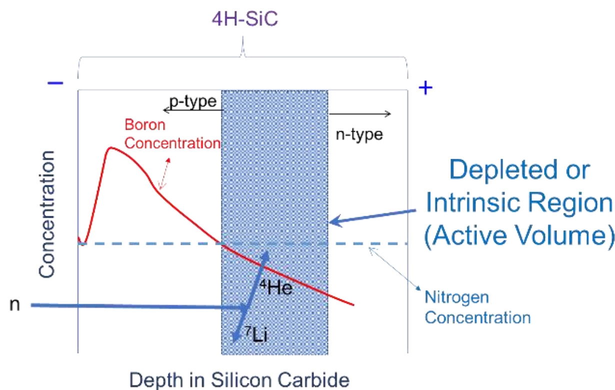

Fig. 3. A thermal neutron can interact with a ^{10}B nucleus within or adjacent to the depleted region to form energetic ^{4}He and ^{7}Li ions, which will produce ionization in the detector active volume.

concentration to avoid excessive neutron attenuation by ^{10}B that is not contributing to the detector response signal.

Therefore, the location and characteristics of the active volume and the detector thermal-neutron sensitivity depend upon several factors:

1. The amount of ^{10}B present.
2. The distribution profile of the boron in the SiC p-n diode.
3. The distance of each ^{10}B atom from the detector active volume.
4. The location and dimensions of the active volume.
5. The extent of attenuation of the thermal neutrons due to the presence of the ^{10}B.

An analysis of the influence of these factors on the observed response of a boron-diffused p-n diode thermal neutron detector follows.

3 The Thermal-Neutron Response of Boron-Diffused SiC Detectors

Fabrication and neutron-response testing of a boron-diffused SiC p-n diode detector were reported at the previous symposium in this series [11]. Secondary Ion Mass Spectrometry (SIMS) measurements of the boron concentration as a function of depth in SiC were reported for the 50-μm detector tested in reference [11]. Two components to the boron concentration profile were observed. A sharp peak with a boron concentration of about (3.5-4.7) x 10^{19} cm^{-3} at a depth of 0.2 μm from the surface was followed by a rapid drop of about a factor of fifty at a depth of approximately 0.26 μm after which a more gradual exponential decrease in concentration occurred up to a depth of 0.8 μm where the measured concentration was (3.9-5.8) x 10^{17} cm^{-3}. Measurement results were not obtained beyond 0.8 μm from the SiC surface. A fit to the boron-concentration data from reference [11] is shown in Figs. 4(a) and 4(b). It can be seen that the boron concentration at a depth of 0.8 μm exceeds the net n-carrier (nitrogen) concentration (~2 x 10^{14} cm^{-3}) by more than a factor of 2000. If a logarithmic extrapolation of the boron concentration is assumed as shown in Fig. 4 (a), the location where the boron and nitrogen concentrations are equal can be estimated as shown in Fig. 4 (b). It can be seen that the boron concentration exceeds the nitrogen concentration up to a depth of 4.8 μm, which corresponds to the location of the p-n interface in the SiC. From the data in Table 1, the maximum $^{10}B(n,\alpha)^{7}Li$ reaction product range is 4.14 μm, and as indicated in Fig. 4 (b), most of the boron atoms in the boron-concentration profile (including the peak) are located where interaction of the neutron-induced reaction products with the detector active volume corresponding to the detector n-region is not possible.

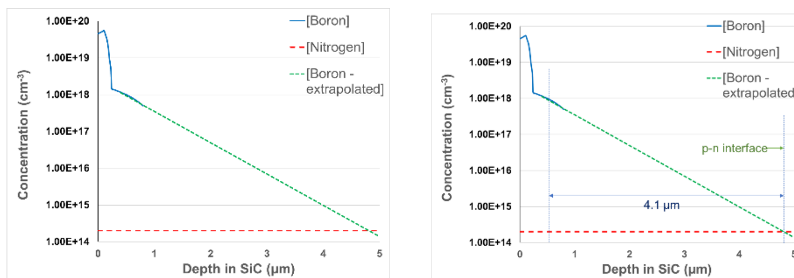

Fig. 4. (a) Measured [11] and extrapolated diffused-boron concentrations in SiC compared to the nitrogen-dopant concentration. **(b)** The p-n interface corresponds to the location where the boron and nitrogen concentrations are equal.

In addition to not effectively contributing to the SiC detector neutron response, the presence of the large concentration of ^{10}B atoms beyond the reaction-product range from the detector active volume will decrease the detector thermal-neutron response due to the high thermal-neutron cross section of ^{10}B (3838 barns) and resulting neutron attenuation.

Also, the extraneous $^{10}B(n,\alpha)^{7}Li$ reactions products will produce radiation damage over time which will reduce the detector service lifetime in high neutron fluence-rate applications.

Therefore, although the boron-diffused SiC detector reported in reference [11] produced a robust response signal, its design was far from optimal. Although it seems counter-intuitive, the first step in optimizing the detector response is to decrease the concentration of the diffused boron.

4 Optimization of the Thermal-Neutron Response of Boron-Diffused SiC Detectors

Initially, an overall reduction in the total boron present by a factor of 120 was assumed. The shape of the boron concentration distribution has been assumed to be unchanged as shown in Fig. 5. The depth of the resulting p-n interface is now 2.4 µm.

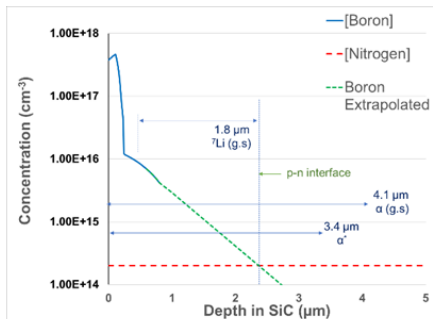

Fig. 5. Boron concentration distribution in SiC assuming a reduction of all boron concentrations by a factor of 120 from those used in the as-built detector configuration.

It can be seen from Fig. 5 that the entire boron concentration is located close enough to the p-n interface to allow the alpha particles from both the ground state (4.1-µm range) and excited state (3.4-µm range) of the $^{10}B(n,\alpha)^{7}Li$ reaction to reach the detector active volume. However, most of the 1.8-µm ^{7}Li ions produced in the $^{10}B(n,\alpha)^{7}Li$ ground-state branch and the 1.6-µm ^{7}Li ions produced in the excited-state branch are not capable of crossing the p-n interface into the detector active volume, because most of the boron-concentration is located within 0.6 µm of the detector surface. Nevertheless, the sensitivity of this reduced boron-concentration detector configuration can be expected to be higher than that of the detector configuration reported in reference [11].

In order to assess the potential neutron sensitivities of the different detector configurations, a crude, two-dimensional model was developed where the sensitivity of the detector was taken to be proportional to a line integral of the products of boron concentration at points along the boron concentration distribution times the corresponding solid angles defined by the range of particles capable of reaching (or passing) the detector p-n interface. Isotropic reaction-product distributions were assumed. It was also assumed that a residual range of at least 1 µm would be needed to produce a sufficient ionization pulse in the detector active volume, and initially, only the 94% excited-state reaction branch was modeled.

The calculations indicate that approximately 0.0235% of the $^{10}B(n,\alpha)^{7}Li$ reactions can contribute to the signal in the detector as fabricated [11], but that roughly 28.6% can contribute if the concentration is reduced by a factor of 120. Therefore, a net increase in

detector neutron sensitivity of roughly a factor of 10 should result if the boron content of the detector is reduced by a factor of 120. This increase results from inclusion in the detector response of more reactions from near the peak of the boron concentration distribution, whereas the original detector response relied on reactions from the low-concentration tail of the distribution.

In order to further increase the detector sensitivity by including the response to ^{7}Li ions and more of the α particles, a configuration where the original boron concentration was reduced by a factor of 1000 was assumed as shown in Fig. 6. It can be seen that the factor

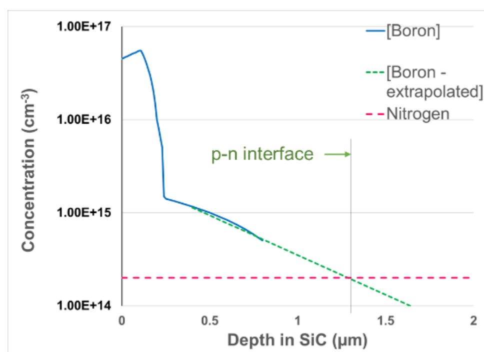

Fig. 6 Boron concentration distribution in SiC assuming a reduction of all boron concentrations by a factor of 1000 from those used in the as-built detector configuration.

of 1000 decrease in the boron concentration distribution has shifted the location of the p-n interface to 1.29 μm. Most of the ^{7}Li ions produced by neutron reactions with the boron distribution are now capable of crossing the p-n interface as are most of the α particles. The calculated fraction of the ^{10}B atoms that can contribute to the signal for this configuration is 68.6%. Therefore, reduction of the boron concentration distribution by a factor of 1000 results in a factor of 2900 times more detector sensitivity or a net sensitivity gain of a factor of 2.9.

The p-n detector configuration resulting from reducing the original boron concentration profile by a factor of 2800 results in a p-n interface that has been shifted further downward to 0.75 μm and the corresponding fraction of the boron concentration that contributes to the detector response increases to 90.1%. The decrease of a factor of 2800 in boron concentration has resulted in a factor of 3800 increase in detector sensitivity, or a net gain of a factor of 1.4.

The p-n detector configuration resulting from reducing the original boron concentration profile by a factor of 5600 results in a p-n interface that has been shifted further downward to 0.41 μm and the corresponding fraction of the boron concentration that contributes to the detector response has increased to 94.8%. The decrease of a factor of 5600 in boron concentration has resulted in a factor of 4830 increase detector sensitivity to the boron present, or a net gain of a factor of 0.7, *i.e.,* there is a net decrease in detector sensitivity by about 30%. Presumably, further decreases in the boron concentration would result in further decreases in net sensitivity, because the detector sensitivity is reaching its theoretical limit of 100% (2π geometry times two ionizing particles per neutron reaction). Therefore, further boron reductions will result in a proportional reduction in neutron sensitivity.

5 Conclusions

The results are summarized in Table 2. It must be emphasized that these results are based on a crude, two-dimensional model, and more precise results should use a more sophisticated three-dimensional model that accounts more precisely for the details of the

boron-concentration distribution. In order to construct such a model, more detailed data are needed for the boron concentrations measured to date as well as information on the net n^- carrier (nitrogen) depth profile. Also, measurements that probe the location of the p-n interface and the depletion depth as a function of reverse bias are needed. In addition, the more detailed model should consider the thermal-neutron attenuation effects of the boron content of the detector on neutron sensitivity.

Table 2. Relative SiC p-n Detector Thermal-Neutron Sensitivities as a Function of Amount of boron Diffused into the Detector

Boron Concentration Distribution	p-n Interface Depth	Percent of Total Boron Contributing to Response	Relative Boron Contribution	Net Relative Increase in Response
Base Case (x1)	4.8 μm	0.0235%	1.00	---
Concentration/120	2.4 μm	28.6%	1220	10.1
Concentration/1000	1.29 μm	68.6%	2920	2.9
Concentration/2800	0.75 μm	90.1%	3830	1.4
Concentration/5600	0.41 μm	94.8%	4030	0.7

Nevertheless, the conclusions obtained with the crude detector-response model demonstrate the trade-off between amount of boron diffused into the detector and detector neutron sensitivity. Clearly, boron concentrations significantly less than originally used [11] are sufficient to produce optimal detector response. Based on the results reported herein, a more optimum detector response will likely be obtained with about a factor of 2000±500 reduction in the amount of boron used.

Boron-diffused 4H-SiC detectors are a promising technology for optimized, application-specific designs of sensitive, radiation-resistant detectors for monitoring and dosimetry in high-temperature environments.

References

1. F. Franceschini and F. H. Ruddy, "Silicon Carbide Neutron Detectors," Chapter 13 in *Properties and Applications of Silicon Carbide*, R. Gerhartd (Ed.), Intech, 2011, pp. 275-296 2011.
2. F. H. Ruddy, A. R. Dulloo, J. G. Seidel, S. Seshadri, and L. B. Rowland, "Development of a Silicon Carbide Radiation Detector," IEEE Trans. Nucl. Sci., **45**, pp. 536-541 1998.
3. F. Nava, G. Bertuccio, A. Cavallini, and E. Vittone, "Silicon Carbide and Its Use as a Radiation Detector," Meas. Sci. Technol., **19**, pp. 102001-1–25 2008.
4. F. H. Ruddy, "Silicon Carbide Radiation Detectors: Progress, Limitations and Future Directions," Materials Research Society Symposium Proceedings, **5761**, pp. 1-12 2013.
5. K. C. Mandal, J. W. Kleppinger, and S. K. Chaudhuri, "Advances in High-Resolution Radiation Detection Using 4H-SiC Epitaxial Layer Devices," Micromachines, 11, 254-1-27 2020.
6. S. K. Chaudhuri and K. C. Mandal, "Radiation Detection Using n-Type 4H-SiC Epitaxial Layer Surface Barrier Detectors," In: Iniewski K. (eds) Advanced Materials for Radiation Detection. Springer, Cham., Chapter 9, pp. 165-182, 2022. https://doi.org/10.1007/978-3-030-76461-6_9 .
7. J. W. Kleppinger, S. K. Chaudhuri, O. Karadavut, and K. C. Mandal, "Role of deep levels and barrier height lowering in current-flow mechanism in 150 μm thick epitaxial n-type 4H-SiC Schottky barrier radiation detectors," Appl. Phys. Lett., **119**, 063502-1-6 2021.

8. F. H. Ruddy, L. Ottaviani, A. Lyoussi, C. Destouches, O. Palais and C. Reynard-Carette, "Silicon Carbide Neutron Detectors for Harsh Nuclear Environments: A Review of the State of the Art," *IEEE Trans. Nucl. Sci.,* **69**, pp. 792-803 2022.
9. F. H. Ruddy and J. G. Seidel, "Effects of Gamma Irradiation on Silicon Carbide Semiconductor Radiation Detectors," IEEE Nuclear Symposium Conf. Record Paper 4179062, pp583-587, 2006.
10. F. H. Ruddy, A. R. Dulloo, and J. G. Seidel, "Study of the Radiation Resistance of Silicon Carbide Radiation Detectors," Trans. Am. Nucl. Soc. **90**, 348, 2004.
11. K. C. Mandal, T. A. Chowdhury, C. Oner, and F. H. Ruddy, "Design and Response Testing of Boron-Diffused Silicon Carbide Neutron Detectors for Dosimetry and Monitoring Applications," in *Reactor Dosimetry: 16th International Symposium*, ASTM STP1608, M. H. Sparks, K. R. Depriest, and D. W. Vehar, Eds., ASTM International, West Conshohocken, PA, 2018, pp. 353–360, http://dx.doi.org/10.1520/STP160820170042
12. A. R. Dulloo, F. H. Ruddy, J. G. Seidel, T. Flinchbaugh, C. Davison, and T. Daubenspeck, "Neutron and Gamma-Ray Dosimetry in Spent-Fuel Radiation Environments, Using Silicon Carbide Semiconductor Radiation Detectors," in *Reactor Dosimetry: Radiation Metrology and Assessment,* ASTM STP 1398, J. G. Williams, D. W. Vehar, F. H. Ruddy, and D. M. Gilliam Eds., 2001, pp. 683-90.
13. T. Natsume, H. Doi, F. H. Ruddy, J. G. Seidel, and A. R. Dulloo, "Spent Fuel Monitoring with Silicon Carbide Semiconductor Neutron/Gamma Detectors*," Journal of ASTM International*, Vol. 3, Online Issue 3, 2006.
14. F. Issa, V. Vervisch, L. Ottaviana, D. Szalkai, L. Vermeeren, A. Lyoussi, A. Kuznetsov, M. Lazar, A. Klix, O. Palais, and A. Hallén, "Improvements in Realizing 4H-SiC Thermal Neutron Detectors," *ISRD 15 – International Symposium on Reactor Dosimetry,* A. Lyoussi (Ed*.),* EPJ Web of Conferences, **106**, 05004, 2016.
15. J. F. Ziegler, and J. P. Biersack. "SRIM-2013 software package," *see* http://www.srim.org (2013).
16. F. Issa, V. Vervisch, L. Ottaviani, D. Szalkai, L. Vermeeren, A. Lyoussi, A. Kuznetsov, M. Lazar, A. Klix, O. Palais, R. Ferone and A. Hallen, "Study of the Stability of 4H-SiC Detectors by Thermal Neutron Irradiation," Mater. Sci. Forum 821-823 pp. 875-878 2015.
17. F. Issa, V. Vervisch, L. Ottaviani, D. Szalkai, L. Vermeeren, A. Lyoussi, A. Kuznetsov, M. Lazar, A. Klix, O. Palais and A. Hallen, "Radiation Silicon Carbide Detectors Based on Ion Implantation of Boron," IEEE Trans. Nucl. Sci. **61**, 2105-2111 2014.
18. F. Issa, L. Ottaviani, D. Szalkai, L. Vermeeren, V. Vervisch, A. Lyoussi, R. Ferone, A. Kuznetsov, M. Lazar, A. Klix and O. Palais, "4H-SiC Neutron Sensors Based on Ion Implanted ^{10}B Neutron Converter Layer," IEEE Trans. Nucl. Sci. **63**, 1976-1980 2016.